There is currently no study available on the effects of reservoir-induced deformations on the performance and stability of offshore platforms. The involved intricate geomechanical processes are of a coupled nature and not yet well understood. In order the obtain a comprehensive understanding of the effects of reservoir deformations on piles, the following geomechanical processes are to be studied in a rigorous manner: (1) coupled pore pressure-deformation variations within the reservoir rock (Atefi Monfared et al., 2016, 2017), (2) geomechanical interactions between reservoir rock and sealing rocks (Atefi Monfared et al., 2015), (3) translation of subsurface deformations to seabed movements, (4) effects of the latter on pile performance.

The objective of this paper is to demonstrate, impacts of reservoir-induced deformations during production and injection operations (i.e. subsidence and upheaval) on the strength of an offshore platform foundation. To achieve this, a numerical model of a single driven pile into a layered media is developed, and calibrated using available data in the literature from a case study on platform EC368A, located in the Gulf of Mexico (Chen et al., 2013). Platform EC368A was chosen in this study for modeling and calibration due to the fact that it is the first documented case of platform failure directly associated with the geomechanical failure of the system of piles.

Next, impacts of seabed subsidence and upheaval induced during hydrocarbon production and injection operations on pile's bearing capacity are analyzed. The rationale adopted is a synthesis of the unidirectional deformation technique (developed from the theory of dislocations), thus assuming the reservoir deformations to be mostly one-dimensional. This is a realistic assumption for geological reservoirs where the thickness is significantly smaller compared to the depth or width (Atefi Monfared et al., 2011). To model reservoir deformations in this study, flow-induced deformations are incorporated within a reservoir rock assumed to be located at a depth of 300 m below the seabed surface. The system of coupled equations developed by Atefi Monfared et al. (2017) are adopted to compute an estimate for induced stress distributions within the reservoir rock due to injection and production flow. The ultimate bearing capacity of the pile is assessed in this paper for three scenarios: (1) trivial subsurface deformations; (2) platform subjected to subsidence; (3) platform subjected upheaval. This assessment demonstrates potential geomechanical effects of production and injection operations on the strength of a single pile. It should be noted that this work provides a foundation for future studies. The numerical model developed in this study has numerous ramifications, and will be adopted in the future to conduct stability assessments of a system of piles in offshore conditions once subjected to subsidence or upheaval. The significances of the geomechanical study presented in the current paper are as follows: (1) development of a numerical model for pile in offshore conditions that has been calibrated versus real data from EC368A case history which represents a large-diameter in-service pile, versus small scale test piles; (2) the developed numerical model incorporates, effects of reservoir-induced deformations on pile capacity in offshore conditions.

PLATFORM EC368A DESCRIPTION

Platform "EC368A" was a three legged, steel jacket platform with a driven, steel pipe foundation located offshore Louisiana in approximately 110 m of water. All three piles were 1.22 m in diameter, open ended and made of A36 steel with two of the piles being double-battered at a 1:5 horizontal to vertical ratio away from the one vertical pile. The vertical pile penetrates 80.8 m into the seabed and the two angled piles penetrate at a depth of 67.1 m. The critically loaded pile that resulted in a 1 meter pull-out failure was one of the angled piles and led to the overturning of the platform by 4°. During installation, the piles were driven in sections as well as welded in the field and the pipe wall thicknesses varied slightly with depth (Chen et al., 2013).

The foundation design for platform EC368A was conducted using the greatest storm load expected during a 100 year span for the area, however, Hurricane Ike exceeded those values. The maximum wave height was about 22 m, 15-20% higher than the design, and the wind speed was approximately 114 km/hr. Failure of the foundation pile was determined to be due to the rapid and cyclic loads from the waves caused by the hurricane. This cyclic loading, along with the degradation of side shear during the pile driving process, caused the soils to weaken through strain-softening which reduced the axial capacity of the platform's foundation. This allowed the pile to be uplifted and resulted in the overturning of the entire platform (Figure 1).

Figure 1. Rotation of Platform EC368A after Hurricane Ike (Energo Engineering, 2010).

NUMERICAL MODEL

FLAC3D from *Itasca* is adopted in this study. The developed model is composed of two main components: (1) pile within a layered medium in offshore conditions; (2) spatial flow-induced deformations due to injection as well as production flow in a confined reservoir layer. The adopted methodology is described in the following text.

Pile Simulation. A vertical pile from platform EC368A, located below a depth of approximately 110m of seawater, with the parameters described earlier in this paper is modeled using FLAC3D. The seabed in which the foundation pile is embedded has a soil profile consisting of two strata. The top 4 m is composed of a "very soft olive gray clay with shell fragments", and is represented in this study with parameter values chosen from a very soft, highly plastic, normally consolidated clay. Below the top 4 m, up to and past the maximum embedment of the pile being analyzed, is a "soft to hard olive gray clay with intermittent silt partings, seams and pockets". The parameter values chosen for this second layer are that of a soft to hard, highly plastic, slightly over consolidated clay. A reservoir layer is assumed at a depth of 300 m below the seabed surface. The commonly used Mohr-Coulomb constitutive model is adopted for all soils.

In order to assess interactions between the pile and the surrounding soil, "interfaces" are adopted. Interfaces in FLAC3D, analogous to the Winkler model, represent a plane on which sliding or separation occurs. Interface is characterized by normal and shear stiffness parameters. Identifying correct values for the aforementioned parameters is a challenge, and continues to be a topic of ongoing research in the current literature. Details regarding the selection of suitable values for these parameters in this study are described in the following section.

The horizontal extension of the selected mesh is chosen far enough to avoid inducing boundary effects on pile-soil interactions. We avoided simulation of an axisymmetric model, as the intension is to develop a more rigorous model to be able to assess effects of various reservoir deformation distributions, which result in different surface response profiles, on pile strength. In order to facilitate run time of the numerical model, for the purpose of this paper, the vertical scale of the mesh was reduced by 1/10th. Therefore, the total pile length is modeled to be 6.71 m. Since the variations in the pile thickness are trivial compared to the dimensions of the simulated model, the average of 0.6 m is selected for the pile radius along the entire length of the pile. The pile is taken to be a uniform solid body, and is assigned average properties computed from the hollow steel casing and the filling soil parameters of the actual case. The reason for this simplification is to avoid further complications, as the focus of this study is not to assess internal interactions between the hollow steel pile casing and the filling soil. A vertical cross section of the geometry mesh is presented in Figure 2. Table 1 presents the adopted input values.

In order to assess the ultimate bearing capacity of the pile, velocities are applied in steps at the grid points located on top of the pile. Axial stress at the top of the pile is monitored and plotted versus the axial displacement, from which the ultimate bearing capacity is obtained. This value is then compared to the value computed and presented from the actual case study. The interface stiffness coefficient parameters are subsequently adjusted so that the bearing capacity of the model matches the actual failure case.

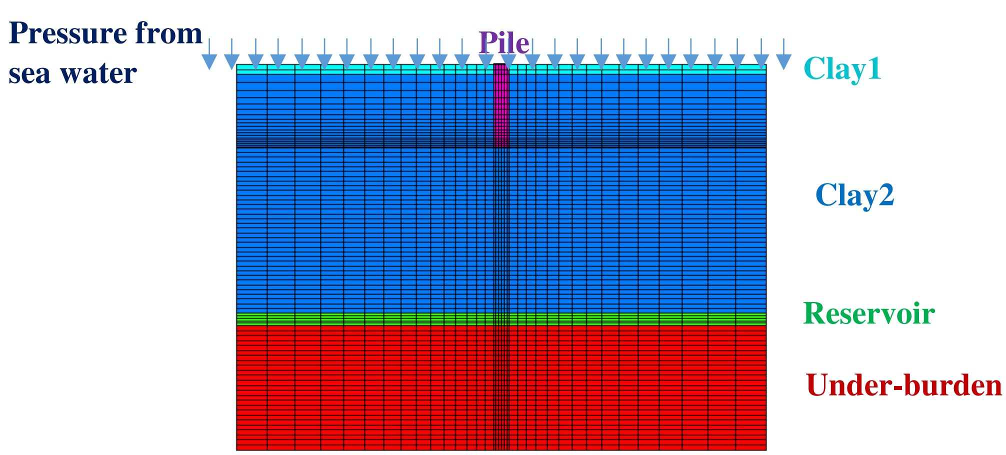

Figure 2. Vertical cross section of the geometry mesh.

Table 1: Model input parameters.

		Pile	Soil #1	Soil #2
Elastic Properties	**ρ**	3,071.3 kg/m^3	1900 kg/m^3	1900 kg/m^3
	E	37.5 GPa	15 MPa	100 MPa
	v	0.285	0.35	0.35
	K	26.07 GPa	16.66 MPa	111.11 MPa
	G	14.875 GPa	5.55 MPa	37.04 MPa
Strength Properties	**c**		20 kPa	150 kPa
	ϕ		10^o	15^o

Soil #1: Up to a depth of 4 m.
Soil #2: Past depth of 4 m.

Determination of Interface Stiffness Coefficients. The Winkler model was adopted in order to properly represent the interaction between the soil and the embedded pile. The following formula was used to obtain an initial estimate for k, the coupled spring stiffness (Mylonakis, 2001).

$$\mathrm{k} \cong 1.3\mathrm{G_s}(\frac{\mathrm{E_p}}{\mathrm{E_s}})^{-0.025} * [1 + 7(\frac{\mathrm{L}}{\mathrm{d}})^{-0.6}]$$

Where the subscripts *s* and *p* correspond to the values of the soil and pile respectively. Since this is a practical estimation of the depth independent spring parameters, the same value is used for the shear and normal spring components in our model. These values are then calibrated via comparing the ultimate bearing capacity of the simulated pile with that of the actual case study.

Flow-induced deformations. ***Injecting*** large volumes of fluids in a confined layer results in an increase in in situ pore pressures, specifically in the vicinity of the injection well. This translates into dilative strains in the soil structure surrounding the well, which in return result in a reduction in pore pressures, bringing about further strain variations. Therefore, there exists a coupling between reservoir's mechanical response and the quantity of the interstitial fluid flow during injection operations. Atefi-Monfared et al.[1], (2017) proposed a series of coupled poroelastic equations to predict the coupled spatiotemporal pore pressures and deformations within a confined porous layer, incorporating effects of vertical confinement. The vertical stress and deformation equation proposed from that study are adopted here to replicate interactions between the injection layer and the surrounding medium.

$$\sigma'_{zz} = \frac{E\alpha Q_o}{4\pi hk} E_1(X) \left[\frac{\left(NY - \frac{1}{F}\right)}{(1+v)} + \frac{v}{(1+v)(1-2v)} \left(Y + NY - \frac{1}{F}\right) \right]$$

$$\varepsilon_{zz} = \frac{\alpha Q_o}{4\pi hk} \left(NY - \frac{1}{F}\right) E_1(X)$$

where σ'_{zz} is the induced stress component in the vertical direction; $E_1(X)$ is exponential integral; $X = cr^2/(4t)$, *c* is the coefficient of diffusivity, *r* the radial distance from injection source, *t* is time from injection initiation; Q_o is injection rate; *h* is the thickness of the injection layer; *N, Y, F* are coefficients based on elastic properties of the injection layer and the vertical confinement. The same rationale stands when analyzing fluid ***extraction*** from a confined porous layer. The coupled system of equations presented by Atefi-Monfared et al.[2], (2017) are adopted to replicate vertical interactions between a production layer and the surrounding medium. A subroutine is written within the numerical model to compute subsurface deformations using the abovementioned equation based on a given Q_o.

In order to estimate flow-induced effects, a typical value is chosen for Q_o. The same value is also adopted as the production rate. Based on Q_o, an estimation of induced deformations within the confined reservoir layer is determined. We assume maximum induced deformations to occur along the center of the pile, to capture the most substantial effects. Figures 3 and 4 present production-induced and injection-induced deformations within the reservoir.

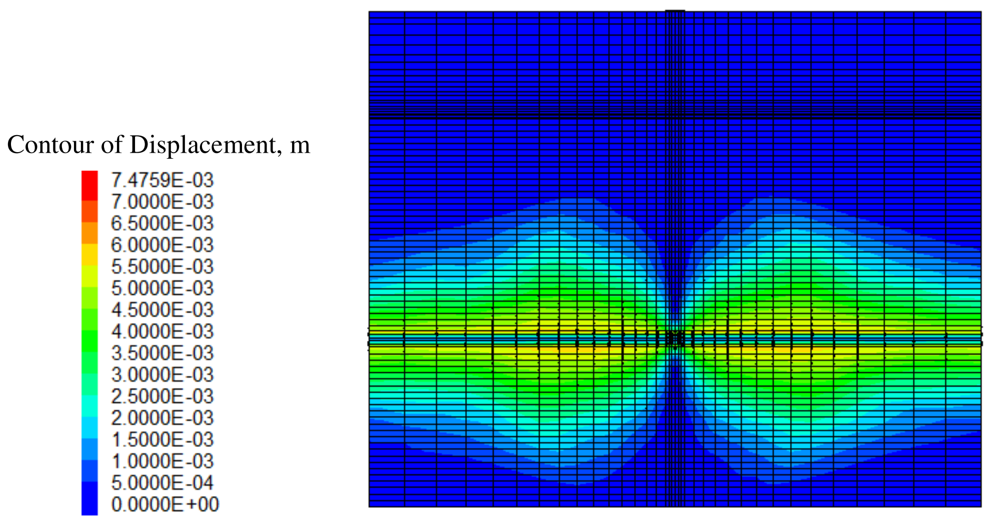

Figure 3. Production-induced deformations.

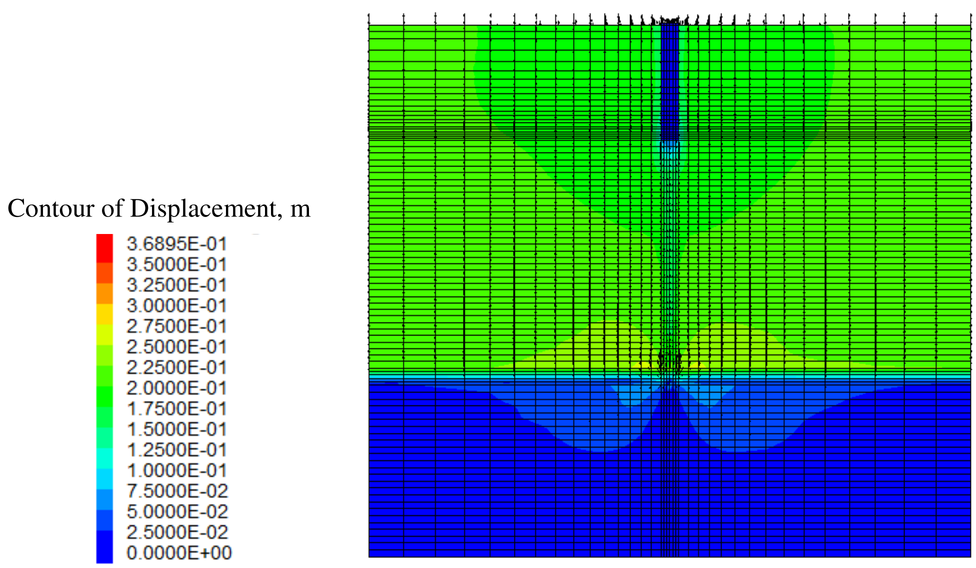

Figure 4. Injection-induced deformations.

It is worth mentioning a famous case of subsidence in the hydrocarbon industry as a reference point for the deformation values adopted in the current study. The Ekofisk oil field was discovered to have subsided approximately 3 m over 11 years. The subsidence basin where most of the platforms are located, sank 6.4 m by 1991 (Nagel, 2001). The rate of subsidence was 30 cm/yr, with the maximum occurring in 1998 at 42 cm/yr (Doornhof et al., 2006). Our chosen values fall way below this critical case.

MODEL CALIBRATION USING ULTIMATE BEARING CAPACITY, Qu

Calculations were done to determine if the ultimate bearing capacity of the full-scale model with our assumed parameter values was within reason of the actual case study. The ultimate bearing capacity is the sum of the skin friction along the pile and the end-bearing capacity at the bottom of the pile (Wrana, 2015).

$$Q_u = Q_b + Q_s$$

$$Q_b = [A_p N_c c_p]$$

$$Q_s = [\sum_{i=1}^{n} \alpha_i c_i A_{si}]$$

$$Q_u = [A_p N_c c_p] + [\sum_{i=1}^{n} \alpha_i c_i A_{si}]$$

Adhesion factors for the soil layers were chosen as 1.0 for the top and 0.39 for the lower soil strata. The first adhesion coefficient was kept at 1.0 for the top soil, the second was determined from Figure 5 for a driven pile overlain by soft clay which is approximately 0.39. c_i is the cohesion of the corresponding clay layer, A_{si} is the area along the pile that is in contact with the surrounding soil. c_p is the cohesion found at the greatest depth along the pile and is equal to the cohesion of the second soil layer which is 150 kPa, N_c is the bearing capacity factor and taken as 9, A_p is the area at the bottom tip of the pile. This results in an end bearing of 1,578 kN and skin friction of 14,455 kN for a pile length of 67.1 meters. The ultimate bearing capacity is thus 16,033 kN. When analyzing the failure of the platform EC368A due to the storm loads brought on by Hurricane Ike, it was determined that the pile's ultimate bearing capacity was close to 16,000 kN, which is in accordance with the above obtained value.

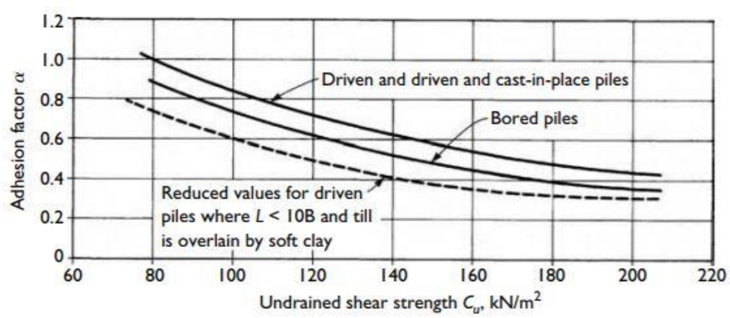

Figure 5. α for bored and driven piles (based on c_u) (Weltman et al., 1978).

It should be emphasized that the pile length in our model was scaled to 1/10th the actual size, with the diameter remaining the same. Also, only half of the pile was modeled due to symmetry of the problem of interest, thus the cross sectional area for determining the bearing capacity load/pressure would be 0.5 of the full cross-section. Using the same adhesion factors as in the full sized foundation pile, the end bearing remains the same, while the skin friction is reduced to 1,357 kN, resulting in an ultimate bearing capacity of 2,935 kN for the simulated pile. This results in an ultimate bearing pressure of 5.1 MPa for modeled cross section. The numerical model was then calibrated through adjusting the normal and shear stiffness values of the interfaces between soil-pile such to obtain a bearing capacity pressure of 5.1 MPa. Bearing capacity is taken as the pressure beyond which a sudden reduction in the load-deflection slope occurs. Figure 6 demonstrates the axial stress-axial displacement curve of the calibrated model which is in a reasonable accordance of the computed value.

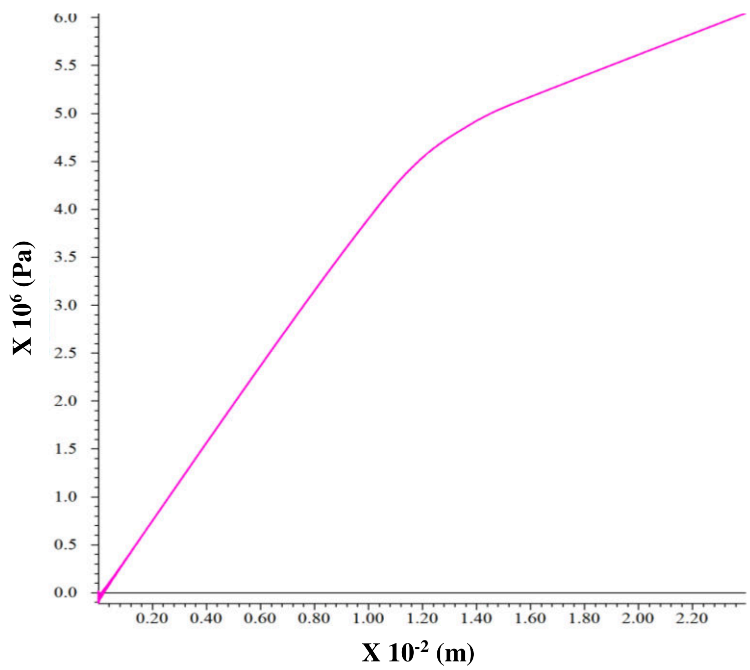

Figure 6. Axial stress versus axial displacement at pile tip, half the cross-section.

RESULTS

The ultimate bearing capacity pressure is the parameter chosen to assess reservoir-induced effects on pile performance in offshore areas. Figure 7 illustrates displacement contours obtained during the axial loading process of the simulated pile in the case of the trivial reservoir deformations. Similar graphs are obtained for cases of reservoir-induced subsidence and upheaval. Figure 8 illustrates axial stress variations versus axial deformations monitored on the top of the simulated pile in cases of subsidence and upheaval within the reservoir layer. The graphs presented in Figure 8 are compared against Figure 6 and briefly discussed in the concluding section.

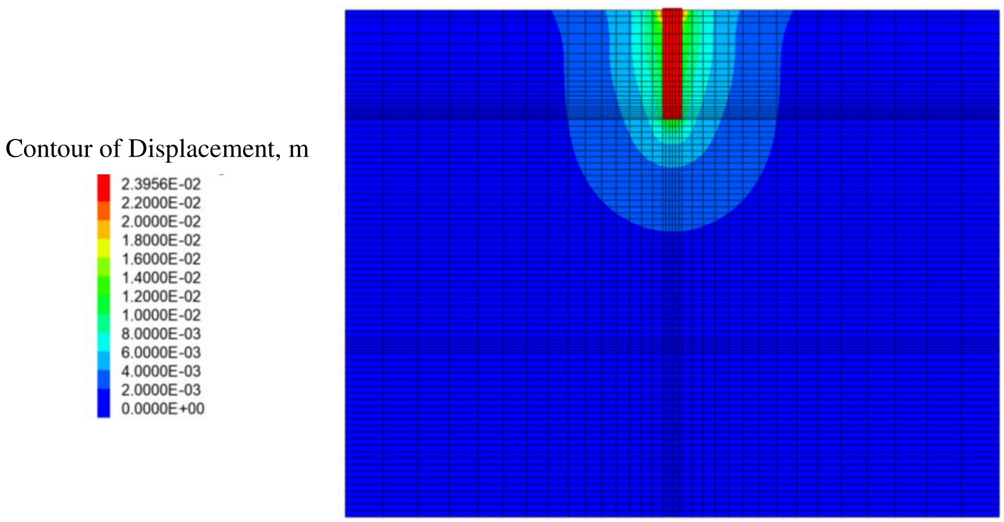

Figure 7. Deformation contour during axial loading of pile (no reservoir deformations).

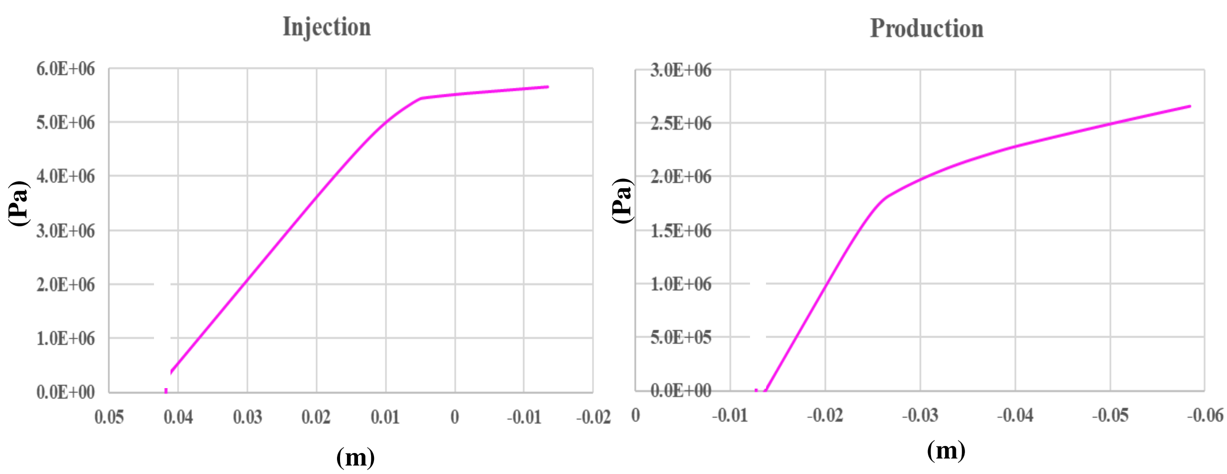

Figure 8. Axial stress versus axial displacement at pile tip, half the cross-section.

DISCUSSION AND CONCLUDING REMARKS

A comparison between Figures 6 and 8 confirms the hypothesis that reservoir induced deformations do in fact significantly affect the bearing capacity of a single pile in offshore conditions. The results suggest that production flow resulted in the ultimate bearing pressure to drop to 1.8 MPa. It should be emphasized that this significant reduction in the pile's bearing capacity occurred as a result of subsidence values (Figure 3) that are far smaller compared to some critical cases (such as Ekofisk). An interesting observation is that injection operations, which resulted in upheaval of the overburden did actually increase the bearing capacity. The volumetric expansion beneath the structure acted as an additional support for the pile, increasing its capacity. It should however be noted that upheaval due to quick injection operations are typically short-term and gravitational forces will reverse these deformations over time.

Results of this study demonstrate the importance of incorporating reservoir-induced geomechanical effects, specifically during production operations, on pile's performance, and thus must be incorporated in the design of offshore platforms. The numerical model developed in this study has numerous ramifications, and will be adopted in a future work to conduct stability assessments of a system of piles in offshore conditions subjected to subsidence and upheaval.

REFERENCES

Atefi Monfared, K., and Rothenburg, L. (2011). "Ground surface displacements and tilt monitoring for reconstruction of reservoir deformations". *Int. J. of Rock Mech. and Mining Sciences*, 48(7), 1113-1122.

Atefi Monfared, K., and Rothenburg, L. (2015). "Poroelastic stress modifications surrounding a fully-penetrating injection well". *J. of Petroleum Science and Eng.*, *135*, 660-670.

Atefi Monfared, K., and Rothenburg, L. (2016). "Poro-elasto-plastic response of an unconsolidated formation confined with stiff seal rocks under radial injection". *Int. J. for Numerical and Analytical Methods in Geomechanics*, 40(13), 1799-1826.

Atefi Monfared, K., and Rothenburg, L. (2017). "Poroelasticity during Fluid Injection in Confined Geological Reservoirs: Incorporating Effects of Seal-Rock Stiffness". *SPE J.*, *22*(01), 184-197.

Chen, J. Y., Gilbert, R. B., Puskar, F. J. and Verret, S. (2013). "Case study of offshore pile system failure in Hurricane Ike". *J. of Geotechnical and Geoenvironmental Eng.*, *139*(10), 1699-1708.

Energo Engineering (2010). "Assessment of damage and failure mechanisms for offshore structures and pipelines in Hurricanes Gustav and Ike." *Rep. MMS TAR* Project No. 642, Minerals Management Service, U.S. Dept. of Interior, Herndon, VA.

Itasca. (1997). FLAC3D Version 6.0, Fast Lagrangian Analysis of Continua in 3 Dimensions. Minneapolis, Minnesota: *Itasca Consulting Group*.

Keszthelyi, D., Dysthe, D. K. and Jamtveit, B. (2016). "Compaction of North-sea chalk by pore-failure and pressure solution in a producing reservoir". *Frontiers in Physics*, 4, p.4.

Mylonakis, G., (2001). "Winkler modulus for axially loaded piles". *Geotechnique*, *51*(5), 455-462.

Nagel, N. B., (2001). "Compaction and subsidence issues within the petroleum industry: From Wilmington to Ekofisk and beyond". *Physics and Chemistry of the Earth, Part A: Solid Earth and Geodesy*, 26(1-2), 3-14.

Doornhof, D., Kristiansen, T. G., Nagel, N. B., Pattillo, P. D. and Sayers, C. (2006). "Compaction and subsidence". *Oilfield Review*, 18(3), 50-68.

Wrana, B., (2015). "Pile load capacity–calculation methods". *Studia Geotechnica et Mechanica*, *37*(4), 83-93.

Weltman, A. J., Healy, P. R. (1978). "Piling in 'boulder clay' and other glacial tills". *Construction Industry Research and Information Association (CIRIA)*, Report PG5.

Lateral Resistance of Piles within Corrugated Metal Sleeves

Dalin N. Russell, M.ASCE[1]; and Kyle M. Rollins, Ph.D., M.ASCE[2]

[1]GeoEngineers, Inc., 11955 Lakeland Park Blvd., Baton Rouge, LA 70809. E-mail: drussell@geoengineers.com
[2]Dept. of Civil and Environmental Engineering, Brigham Young Univ., Provo, UT 84604. E-mail: rollinsk@byu.edu

Abstract

Pile foundations supporting bridge abutments are often driven inside corrugated metal pipe sleeves (CMS) which extend through the approach fill to reduce downdrag or for construction expediency. The annular space between the pile and the sleeve is typically filled with uncompacted pea gravel. Designers often assume that the lateral resistance of the pile within the sleeve will be minimal; however, no test results are available to confirm this assumption. To investigate the lateral resistance of piles driven within CMS, a full-scale lateral load test was performed. The test pile configuration included a 32.4 cm (12.75 in.) pipe pile within a 60 cm (24 in.) CMS with uncompacted pea gravel filling the annular space. Results indicate that after small pile displacements, the lateral pile resistance was similar to that provided by an individual pipe pile and was even greater at larger displacements. As the pile displaced laterally, the gravel within the annular space became engaged and displaced the CMS into the compacted fill. Back-analyses indicate that the ultimate lateral pile resistance for this case can be approximated by treating the pipe-gravel-CMS as a composite pile having an EI equal to the pipe pile but with a diameter equal to the CMS.

INTRODUCTION

Pile foundations supporting bridge abutments are often driven inside corrugated metal pipe sleeves (CMS) which extend through the approach fill. These sleeves may be used to reduce downdrag from settlement of the approach fill or simply to preserve a hole through a Mechanically Stabilized Earth (MSE) fill so that construction of the fill can commence before the pile is driven. Typically, the annular space between the CMS and the pile is back-filled with uncompacted sand or pea gravel. For piles supporting integral abutments, the pile-sleeve methodology is meant to provide reduced stiffness for lateral loading of piles while reducing the potential for buckling under axial load. Because these sleeves are placed near the head of the